

# Critical interaction of a shock wave with an acoustic wave

Jean-Christophe Robinet<sup>a)</sup>

ONERA-CERT, Aerodynamics and Energetics Modeling Department, 2, Avenue Edouard Belin, B.P. 4025, 31055 Toulouse Cedex 4, France

Grégoire Casalis<sup>b)</sup>

ONERA-CERT, Aerodynamics and Energetics Modeling Department, 2, Avenue Edouard Belin, B.P. 4025, 31055 Toulouse Cedex 4, France  
and Ecole Nationale Supérieure de l'Aéronautique et de l'Espace, 10, Avenue Edouard Belin, 31400 Toulouse, France

(Received 28 April 2000; accepted 8 January 2001)

The interaction of linear waves with normal or oblique shock waves has been studied by Moore [NACA Report No. 1165 (1954)], Ribner [AIAA J. **23** (1984)], and McKenzie and Westphal [Phys. Fluids **11**, 2350 (1968)] by writing the fluctuating quantities as normal modes. These different studies have shown that downstream of the shock exists a critical angle of the incident acoustic waves where the reflection coefficient is equal to 1. The purposes of this paper are first to point out that this critical angle may appear as a singularity in the linearized Euler equations, and second to show that this problem can actually be removed if the perturbation is no longer assumed to be a normal mode but has a mathematical form which is strictly deduced from the mathematical nature of the linearized Euler equations. This analysis is then applied to the shock wave oscillations occurring on a wing profile and in a nozzle. Despite many simplifications, good results are obtained in comparison with the available experimental data. © 2001 American Institute of Physics. [DOI: 10.1063/1.1351548]

## I. INTRODUCTION

Most of the applications in fluid dynamics involve unsteady flows. This is also true when a strong shock is present in the flow separating a supersonic flow from a subsonic one. In such cases, the unsteady behavior is usually not wished and must be either eliminated or at least limited (in amplitude). Such undesirable oscillations occur under some conditions for flows in a rocket motor and on transonic airfoils and may lead to the well-known buffeting problem.

In the field of space engines, with the development of large rocket motors, unsteady transverse forces not envisaged before have been observed for ten years. This problem, observed in several engines, has been called "side loads" ever since. Owing to their randomness, these side loads may have serious consequences, such as nozzle deformations and engine movements. Moreover, as the perturbation is unsteady in module and in direction, the resulting constraints may be amplified by dynamic effects. The lateral forces can be thus a limiting factor in the structural design of the nozzle: they impose thicker nozzles, then heavier ones, or shorter nozzles, then less efficient. Both cases lead to a reduction in the payload. The exact cause of this symmetry loss is, however, badly known today; several assumptions have been proposed but without any consensus.

In the field of aircraft, a similar phenomenon occurs above the wing when the plane is close to its flight envelope limit: the buffeting phenomenon. It appears when the angle of attack or the Mach number increases. Although the buf-

feting is characterized by the vibration of the aircraft structure, its origin seems to be purely aerodynamic. In particular, it may result from an unsteady separation located on the airfoil, the vibrations of the structure being produced by a coupling effect. This phenomenon can appear in all flight regimes, it is accentuated for transonic flows by the shock wave oscillations. This phenomenon is not critical for the aircraft but it limits the flight envelope of the civil aircraft, indeed the maximum level of buffeting is fixed by the regulation of the civil aviation.

Although these phenomena are *a priori* very different from the industrial point of view, the involved physical mechanisms seem to be comparable. However, in both cases, the actual flow is somehow complex: presence of a nonzero pressure gradient, a shock wave, a large separation bubble, and unsteadiness. A complete computation does not seem to be realistic nowadays and in addition even if it was feasible, it would only describe the flow, whereas our goal is to understand the origin of the unsteadiness.

A large amount of work has been done and published in the last 50 years with approaches that are mainly numerical or experimental. Recently, a linearized numerical approach, see Ref. 1, provided satisfactory results in comparison with the available experiment, but once more, it does not really help to understand the relevant mechanism.

In our opinion, it seems necessary to come back to simple configurations even if they are not fully realistic. The equations can be then simplified, the resolution may be thus analytical, leading accordingly to a possible identification of the role of the different involved parameters. Our starting point is the study of the linear interaction of an acoustic

<sup>a)</sup>Electronic mail: jrobinet@onecert.fr

<sup>b)</sup>Electronic mail: casalis@onecert.fr

wave with a shock wave. It has been treated by several authors, in particular Moore,<sup>2</sup> Ribner,<sup>3</sup> McKenzie and Westphal,<sup>4</sup> and Mahesh *et al.*<sup>5</sup>

The general objectives of this paper are first to study the linear interaction of a shock wave with an acoustic perturbation and second to show that the shock oscillations in a nozzle or on an airfoil can be surprisingly and simply explained by the shock wave–acoustic wave interaction theory. Basically, two cases depending on the incident angle of this acoustic perturbation appear. Below the so-called critical angle, classical results are briefly recollected. At the critical angle, the linear interaction theory is completely revisited.

The present paper is divided in two main parts. The first part deals with the theoretical description of the proposed approach. After the chosen assumptions (Sec. II A), the theoretical model is described in Secs. II B–II H. In particular, Sec. II E shows that there are singular values of the transverse wave number  $k_y$  for which the linearized Euler equations exhibit non-normal solutions. Section II G briefly presents the results when the wave number  $k_y$  is different from the singular values, this case has been already treated by McKenzie and Westphal.<sup>4</sup> Section II H, devoted to the particular case of the singular values of the wave number  $k_y$ , contains our original contribution. The present theory is then applied in the second part to the practical cases of the shock wave oscillation in a nozzle and on an airfoil wing. It is shown that the singular value of  $k_y$  seems to play an important role.

## II. THEORETICAL PART

### A. Study context: Presentation of the problem and assumptions

We consider a two-dimensional unsteady flow with a straight shock wave. The  $x$  coordinate coincides with the normal of the shock and the  $y$  coordinate is perpendicular to it. The undisturbed shock front is located at  $x=0$  and the flow moves from the  $x<0$  region to the  $x>0$  region. The upstream quantities (supersonic zone) are denoted by subscript 0 and the downstream quantities (subsonic zone) by subscript 1. The flow is considered as a perfect, inviscid gas. The assumptions of the present problem are the following ones:

- The shock is supposed to be sufficiently strong so that the boundary layer downstream of the shock is separated. It is then assumed that this large separation bubble is a source of fluctuations, the maximum being located at the reattachment point, see Ref. 6.
- The radiated waves and the resulting perturbations are supposed to have small amplitudes. The resulting shock displacement is also supposed to be small.
- The radiated waves are supposed to be plane waves, i.e., crests perpendicular to  $\mathbf{k}$ .
- In order to calculate explicitly the shock displacement and the oscillation frequency  $\omega$ , the value of the pressure fluctuation is imposed by assuming that the reattachment point is an antinode of pressure fluctuation. This is a crude assumption.

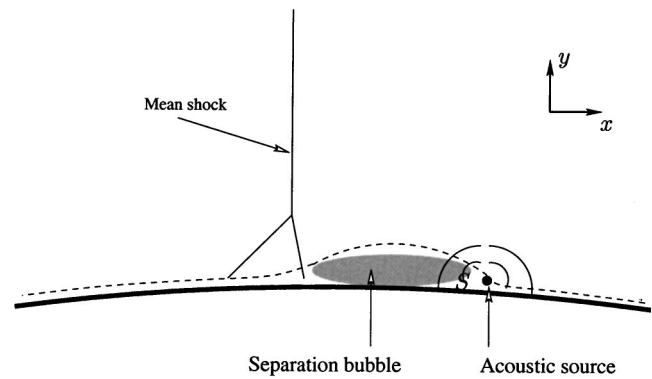


FIG. 1. Physics of the problem.

- The supersonic zone is supposed to be free of any perturbation.

Figure 1 presents the physics of the considered problem.

### B. Governing equations and boundary conditions

The general equations for the instantaneous flow are the Euler equations, the energy equation, written for the entropy, and the equation of state for a perfect gas:

$$\frac{\partial \rho}{\partial t} + \nabla \cdot (\rho \mathbf{U}) = 0, \quad (1a)$$

$$\rho \frac{\partial \mathbf{U}}{\partial t} + \rho (\mathbf{U} \cdot \nabla) \mathbf{U} = -\nabla P, \quad (1b)$$

$$\frac{\partial S}{\partial t} + (\mathbf{U} \cdot \nabla) S = 0, \quad (1c)$$

$$S = C_v \ln \left( \frac{P}{\rho^\gamma} \right), \quad (1d)$$

where  $\mathbf{U} = (U, V)^t$  represents the two mean velocity components. In addition to these equations, the instantaneous Rankine–Hugoniot shock relations are imposed at the instantaneous shock position (see Sec. II D). The governing equations and the Rankine–Hugoniot relations form the physical system to be solved. The boundary condition of this problem is a given fluctuation radiated from a given point. In the considered applications, Sec. III, the boundary condition is a plane acoustic wave radiated from the reattachment point of the separation bubble.

### C. Mathematical form of the perturbation

The present theory is based on the classical small perturbations technique, the instantaneous flow being the superposition of a known mean flow and unknown fluctuations. All the physical quantities  $q$  (for example, velocity components, pressure, etc.) are thus decomposed into a mean value and a fluctuating one:

$$q(x, y, t) = \bar{q} + q_f(x, y, t). \quad (2)$$

The mean value  $\bar{q}$  is assumed to be a constant in the  $(x, y)$  plane on each side of the shock. This implies that in fact two

decompositions are written: one upstream of the shock, the other one downstream. According to the constant form of the mean flow, the perturbation can be described as a normal mode with respect to the different variables  $y, t$ :

$$q(x, y, t) = \bar{q} + \tilde{q}(x) e^{i(k_y y - \omega t)} + \text{c.c.}, \tag{3}$$

where  $\tilde{q}(x)$  is the amplitude of the fluctuations,  $k_y$  is a transverse wave number with  $k_y \in \mathbb{R}$ , and c.c. denotes the complex conjugate. The circular frequency  $\omega$  is a real number, it represents the frequency of the phenomenon. The mean flow being constant on both sides shock,  $\tilde{q}(x)$  can be written in the normal mode form  $e^{ik_x x}$ , see Sec. II E. This more general expression is used for the treatment of the shock relations. In the following section,  $e^{i(k_y y - \omega t)}$  is noted  $E$ .

### D. Linearized Rankine–Hugoniot relations

The same small perturbation technique (2) is used for the shock equations (for more details see Ref. 7). The perturbed position of the shock is written as

$$x = f(y, t) = \bar{x}_c + XE + \text{c.c.}, \tag{4}$$

where  $\bar{x}_c$  is the mean shock position (here,  $\bar{x}_c = 0$  due to the choice of the coordinate system) and  $X$  represents the shock oscillation amplitude. The latter is assumed to be a small (complex) quantity. The Rankine–Hugoniot relations are then linearized by performing a first-order Taylor expansion with respect to the shock displacement amplitude  $X$ . Each quantity,  $q_j$ ,  $j = 0, 1$  is the sum of the mean quantity and the fluctuating quantity, both being evaluated just upstream ( $j = 0$ ) or downstream ( $j = 1$ ) of the perturbed shock position.  $q_j$  is expressed as

$$q_j(\bar{x}_c + XE, y, t) = \bar{q}_j(\bar{x}_c + XE) + q_{j,j}(\bar{x}_c + XE, y, t), \tag{5}$$

$$j = 0, 1.$$

As the coordinate system is such that  $\bar{x}_c = 0$ ,  $q_1$  and  $q_0$  are expanded into

$$q_j(XE, y, t) = \bar{q}_j(0) + \check{q}_j(0)E \quad \text{for } j = 0, 1, \tag{6}$$

where  $\check{q}(0)$  is the amplitude of the fluctuation at the mean shock position. After some calculations, the linearized shock relations lead to an algebraic system of equations:

$$\mathbf{A}_1 \mathbf{Z}_1(0) = \boldsymbol{\xi} X + \mathbf{A}_0 \mathbf{Z}_0(0), \tag{7}$$

where  $\mathbf{Z}_j(0)$  (for  $j = 0, 1$ ) stands for the fluctuating amplitudes vector  $(\check{p}, \check{u}, \check{v}, \check{s})$  calculated at the mean shock position.  $\boldsymbol{\xi}$  is a known complex vector and  $\mathbf{A}_0, \mathbf{A}_1$  are fourth-order known complex matrices. For a one-dimensional constant flow on both sides of the shock, the general linearized Rankine–Hugoniot, Eq. (7), can be simplified into

$$\left[ \frac{\bar{U}}{\bar{c}^2} \check{p} \right] + [\bar{\rho} \check{u}] - \frac{\bar{\rho} \bar{U}}{C_p} [\check{s}] - i \omega \bar{\rho}_1 \frac{[\bar{U}]}{\bar{U}_0} X = 0,$$

$$\left[ \left( 1 + \frac{\bar{U}^2}{\bar{c}^2} \right) \check{p} \right] + 2 \bar{\rho} \bar{U} [\check{u}] - \left[ \frac{\bar{\rho} \bar{U}^2}{C_p} \check{s} \right] = 0, \tag{8}$$

$$\left[ \frac{1}{\bar{\rho}} \check{p} \right] + [\bar{U} \check{u}] + \left[ \frac{\bar{c}^2}{C_p (\gamma - 1)} \check{s} \right] + i \omega [\bar{U}] X = 0,$$

$$[\check{v}] + i k_y [\bar{U}] X = 0,$$

where  $[q] = (q_0 - q_1)$  indicates the jump relation at the mean shock location of the quantity  $q$ .

### E. Linearized Euler equations

The decomposition (3) is introduced into Eqs. (1a)–(1d). The resulting equations are then simplified, first by taking into account that the mean quantities satisfy the equations and second by assuming that the fluctuating quantities are small, so that these equations can be linearized with respect to the disturbance. The resulting equations constitute an ordinary differential equations system with respect to  $x$  and with constant coefficients. Thus, the solution can be sought under an exponential  $x$  dependence:  $\tilde{q}(x) = \hat{q} e^{ik_x x}$ , where  $k_x$  is the longitudinal wave number downstream of the shock. It is appropriate to specify that  $\check{q}$  represents the global fluctuation whereas  $\hat{q}$  (introduced in the previous section) represents the amplitude function associated with the fluctuation written in the normal modes form. Finally, the linearized Euler equations become a homogeneous algebraic system:

$$(\mathbf{M} - k_x \mathbf{N}) \mathbf{Z} = 0, \tag{9}$$

where  $k_x$  appears as the eigenvalue of the problem.  $\mathbf{Z}$  stands for  $(\check{p}, \check{u}, \check{v}, \check{s})$  and  $\mathbf{M}$  and  $\mathbf{N}$  are  $(4 \times 4)$  matrices which depend on the mean flow and of the coefficients  $\omega$  and  $k_y$ . For the explicit form of matrices  $\mathbf{M}$  and  $\mathbf{N}$ , see Ref. 8.

A nonzero solution in Eq. (9) exists if  $\det(\mathbf{M} - k_x \mathbf{N}) = 0$ . This condition provides four different wave numbers:

$$k_x^{(1)} = \frac{-\omega \bar{U}_1 - \bar{c}_1 \Omega}{\bar{c}_1^2 - \bar{U}_1^2}, \quad k_x^{(2)} = \frac{-\omega \bar{U}_1 + \bar{c}_1 \Omega}{\bar{c}_1^2 - \bar{U}_1^2},$$

$$k_x^{(3)} = k_x^{(4)} = \frac{\omega}{\bar{U}_1}, \tag{10}$$

where  $\Omega = [\omega^2 - k_y^2 (\bar{c}_1^2 - \bar{U}_1^2)]^{1/2}$  and  $\bar{c}_1 = (\gamma r \bar{T}_1)^{1/2}$ .

The corresponding eigenvectors are

$$\mathbf{V}_{1,2} = [-\bar{\rho}_1 (\bar{U}_1 k_x^{(1,2)} - \omega), k_x^{(1,2)}, k_y, 0]^t,$$

$$\mathbf{V}_3 = [0, k_y, -k_x^{(3)}, 0]^t, \quad \mathbf{V}_4 = [0, 0, 0, 1]^t. \tag{11}$$

$\mathbf{V}_j$  is the eigenvector downstream of the shock. These eigenvectors form a basis if the determinant of the matrix  $\mathbf{M}_v$ , whose columns are the four eigenvectors  $\mathbf{V}_1, \mathbf{V}_2, \mathbf{V}_3, \mathbf{V}_4$ , is different from zero. A straightforward calculation leads to

$$\det \mathbf{M}_v \neq 0 \Leftrightarrow \omega \neq \{ \pm i k_y \bar{U}_1, \pm k_y (\bar{c}_1^2 - \bar{U}_1^2)^{1/2} \}. \tag{12}$$

Physically, the relation  $\omega = \pm ik_y \bar{U}_j$  implies that the second acoustic mode has the same phase speed (wave number) as the vorticity mode (see Ref. 7). On the other hand,  $\omega = \pm k_y (\bar{c}_1^2 - \bar{U}_1^2)^{1/2}$ , implies that the two acoustic modes coincide. However, the first relation may be disregarded because the circular frequency  $\omega$  is required in the present study to be real. It remains the second relation which will be extensively studied in Sec. II H. Let us assume now that condition (12) is satisfied, so that the general solution of Eq. (9) can be written as

$$\mathbf{q}_f = \left( \sum_{j=1}^4 C_j \mathbf{V}_j e^{ik_x^{(j)} x} \right) e^{i(k_y y - \omega t)}. \quad (13)$$

The four coefficients  $C_j$ ,  $j=1, \dots, 4$ , are unknown integration constants downstream of the shock. They are related to the two acoustic waves ( $j=1, 2$ ), the vorticity wave ( $j=3$ ), and the entropy wave ( $j=4$ ), respectively. Finally, the fluctuating quantities are written as

$$\begin{aligned} p_{1_f} &= (-C_1 \bar{\rho}_1 (\bar{U}_1 k_x^{(1)} - \omega) e^{ik_x^{(1)} x} \\ &\quad - C_2 \bar{\rho}_1 (\bar{U}_1 k_x^{(2)} - \omega) e^{ik_x^{(2)} x}) E, \\ u_{1_f} &= (C_1 k_x^{(1)} e^{ik_x^{(1)} x} + C_2 k_x^{(2)} e^{ik_x^{(2)} x} + C_3 k_y e^{ik_x^{(3)} x}) E, \\ v_{1_f} &= (C_1 k_y e^{ik_x^{(1)} x} + C_2 k_y e^{ik_x^{(2)} x} - C_3 k_x^{(3)} e^{ik_x^{(3)} x}) E, \\ s_{1_f} &= C_4 e^{ik_x^{(4)} x} E. \end{aligned} \quad (14)$$

Let us recall that  $E = e^{i(k_y y - \omega t)}$ . In this paper, only the case where the upstream fluctuating quantities are supposed to be zero is treated:  $q_{0_f} \equiv 0$ . See Ref. 8 for the general case.

**F. Global problem resolution**

At this stage, we suppose that the constant  $C_1$  is known, this coefficient corresponds to the incident wave. Substituting expressions (14) at  $x=0$  into the shock relations (8) leads to an algebraic system:

$$\mathbf{G}\boldsymbol{\chi} = \mathbf{F}, \quad (15)$$

where  $\boldsymbol{\chi} = (C_2, C_3, C_4, X)^t$  is the unknown vector,  $\mathbf{G}$  is a fourth-order matrix, which depends on  $\omega$  and  $k_y$  and on the

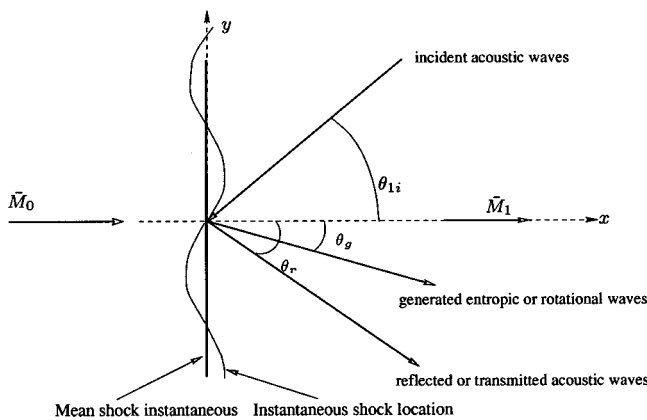


FIG. 2. Drawing of the different considered angles.

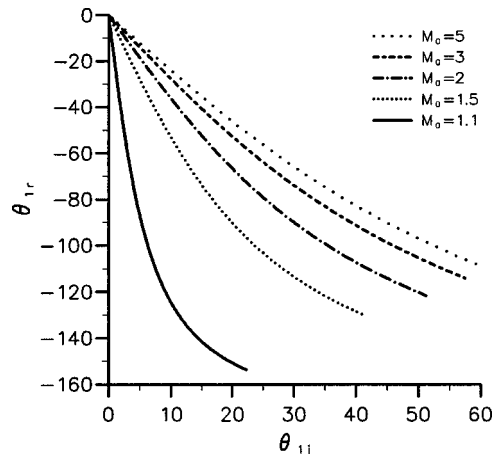


FIG. 3. Angle of the reflected acoustic wave  $\theta_r$  vs  $\theta_i$ .

mean flow values, and  $\mathbf{F}$  is a known source vector (see Appendix A).

The resolution of the system (15) provides the ratio  $C_j/C_1$ ,  $j=2, 3, 4$ . These ratios determine the reflection and generation coefficients of the different waves interacting with the shock as well as the amplitude of the shock displacement.

The objective of this paper is not the systematic investigation of the shock wave response to a linear forcing but only the investigation of a particular configuration. This systematic study has been already achieved by Moore,<sup>2</sup> McKenzie and Westphal,<sup>4</sup> Ribner,<sup>3,9</sup> and Hardy and Atassi.<sup>10</sup> We just focus on the case of an acoustic wave propagating upstream in the subsonic zone and interacting with the shock wave.

**G. Downstream acoustic disturbance**

Let us note  $\theta_{i1}$  and  $\theta_{r1}$  the angles between the wave vectors and the  $x$  direction for, respectively, the incident acoustic wave and the reflected acoustic wave:

$$\theta_{i1} = \arctan\left(\frac{k_y}{k_x^{(1)}}\right), \quad \theta_{r1} = \arctan\left(\frac{k_y}{k_x^{(2)}}\right).$$

It is appropriate to recall that  $k_x^{(1)}$  is negative, the corresponding wave propagates upstream, whereas  $k_x^{(2)}$  is positive, the associated wave thus propagates downstream. Figure 2 shows a drawing of different considered angles. The angle of the reflected wave is shown in Fig. 3 as function of  $\theta_{i1}$  for different Mach numbers  $\bar{M}_0$ . It can be observed that for each Mach number, a threshold value  $\theta_{ic}$  of  $\theta_{i1}$  exists. For  $\theta_{i1} < \theta_{ic}$ , the reflected acoustic wave propagates downstream. Beyond this critical angle  $\theta_{ic}$ , the acoustic wave cannot be propagated without damping or amplification because the longitudinal wave numbers  $k_x^{(1,2)}$  become complex numbers. Moreover, there is an angle  $\theta_{ip}$  beyond which  $|\theta_r|$  is larger than  $\pi/2$ . This angle corresponds to the case for which the reflected vector wave is directed to the shock. The calculation of the phase velocity and the group velocity of the incident wave and the reflected wave permits us to deter-

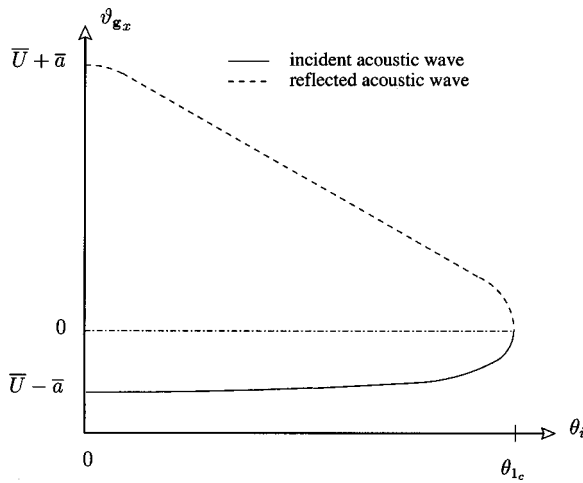


FIG. 4. Longitudinal group velocity  $v_g$  for the incident and reflected acoustic waves vs  $\theta_i$ .

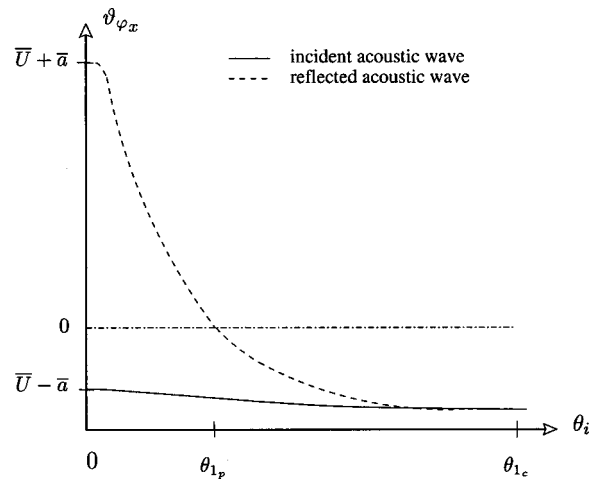


FIG. 5. Longitudinal phase velocity for the incident and reflected acoustic waves  $v_\phi$  vs  $\theta_i$ .

mine the behavior of the acoustic waves according to the incident angle. These velocities are defined as follows:

$$v_\phi = \frac{\omega}{\|\mathbf{k}\|^2} \mathbf{k}, \quad v_g = \frac{\partial \omega}{\partial \mathbf{k}} = \bar{c} \frac{\mathbf{k}}{\|\mathbf{k}\|} + \bar{\mathbf{U}}, \quad (16)$$

for the phase velocity and the group velocity, respectively. Figures 4 and 5, respectively, show the evolution of the streamwise component of the group velocity and the streamwise component of the phase velocity versus the incident angle  $\theta_i$ . Figures 4 and 5 show that the longitudinal phase and the longitudinal group velocity of the incident acoustic wave are always negative. For the reflected acoustic wave, the longitudinal phase velocity is positive if  $\theta_i < \theta_{ip}$  and negative if  $\theta_i \geq \theta_{ip}$ , whereas the longitudinal group velocity is always positive. However, the latter is zero for the two waves when  $\theta_i = \theta_{ic}$  (the transverse group velocity is different from zero at this angle). In conclusion, when  $\theta_i < \theta_i < \theta_{ic}$ , although the wave number is directed to the shock, the

reflected acoustic wave propagates from upstream to downstream. When  $\theta_i = \theta_{ic}$ , the incident and the reflected acoustic wave cannot be distinguished. This angle  $\theta_{ic}$  is given by  $\theta_{ic} = \arcsin(\bar{M})$  and corresponds to the critical transverse wave number  $k_y^c = \omega / \sqrt{\bar{c}^2 - \bar{U}^2}$ . Figure 6 provides a schematic representation of the cone for the admissible (real) propagation directions of the acoustic waves. For more details, see Appendix B. This critical mode corresponds to a value of  $\omega$  which has been excluded, see relation (12) in Sec. II E, a special analysis is thus necessary, see Sec. II H. Before detailing this case, let us look at the evolution of the reflection coefficient to incident acoustic wave versus the incident angle when  $\theta_i < \theta_{ic}$ :

$$\frac{\bar{p}_1^{(r)}}{\bar{p}_1^{(i)}} = \left( \frac{k_x^{(2)} \bar{U}_1 - \omega}{k_x^{(1)} \bar{U}_1 - \omega} \right) \frac{C_2}{C_1}.$$

After some calculations, the pressure ratio can be written as

$$\frac{\bar{p}_1^{(r)}}{\bar{p}_1^{(i)}} = - \left( \frac{k_x^{(2)} \bar{U}_1 - \omega}{k_x^{(1)} \bar{U}_1 - \omega} \right) \left[ \frac{2 \frac{\bar{U}_1}{\bar{U}_0} \omega \left( k_y^2 + \frac{\omega^2}{\bar{U}_1^2} \right) - \left( \frac{\omega^2}{\bar{U}_1 \bar{U}_0} + k_y^2 \right) (\omega - \bar{U}_1 k_x^{(1)}) \left( \frac{\bar{M}_0^2 - 1}{\bar{M}_0^2} \right)}{2 \frac{\bar{U}_1}{\bar{U}_0} \omega \left( k_y^2 + \frac{\omega^2}{\bar{U}_1^2} \right) - \left( \frac{\omega^2}{\bar{U}_1 \bar{U}_0} + k_y^2 \right) (\omega - \bar{U}_1 k_x^{(2)}) \left( \frac{\bar{M}_0^2 - 1}{\bar{M}_0^2} \right)} \right]. \quad (17)$$

Figure 7 shows this evolution for different upstream Mach numbers. This pressure ratio is always lower than 1, the shock can be thus considered as stable in the sense that the amplitude of the reflected wave is always lower than the amplitude of the incident wave. However, this pressure ratio strongly depends on the incident angle. There are angles for which the pressure ratio is zero. When  $\theta_i \rightarrow \theta_{ic}$ , the pressure ratio tends to be maximal and equal to 1 (in absolute value).

In addition, the work of McKenzie and Westphal<sup>4</sup> and Navier–Stokes computations of Zang and Bushnell<sup>11</sup> have shown that in the vicinity of this critical angle, the reflected coefficient of an acoustic wave is close to 1, a result which is in agreement with the previous computations. By extrapolating the results for  $\theta_i \rightarrow \theta_{ic}$ , it can be summarized that: the streamwise component of the group velocity tends to 0 and the reflected wave amplitude becomes identical to that of the

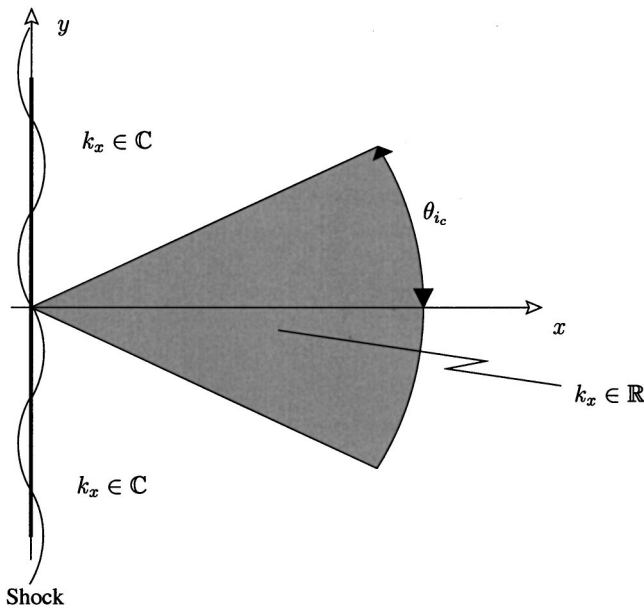


FIG. 6. Diagram representing the critical angle.

incoming one, the shock response becomes marginal. However, as mentioned above, the previous analysis must be performed again from Sec. II E by writing the disturbance in an adapted basis for  $\theta_i = \theta_{i_c}$ . The shock treatment does not need to be analyzed again, because the fluctuation form  $\tilde{q}(0)$  is completely general, independent of its mathematical expression.

**H. Study of critical angle**

Equation (15) has been obtained for  $k_y < \omega/\beta$ , with  $\beta = \sqrt{\bar{c}_1^2 - \bar{U}_1^2}$ , or for  $\theta_i < \theta_{i_c}$ . Let us look at the case  $k_y = \omega/\beta$ , this value corresponds to a value of  $k_y$  which has been excluded and for which the four eigenvectors (11) do not form a basis (12).

For  $k_y = \omega/\beta$ , the eigenvalues of Eq. (9) are given by

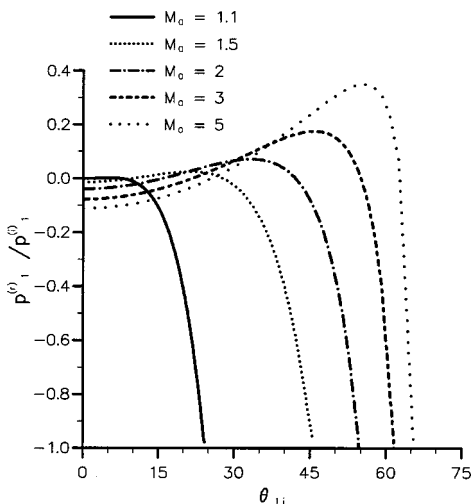


FIG. 7. Angular dependence of the reflection coefficient for acoustic waves for different upstream Mach numbers.

$$k_x^{(1)} = k_x^{(2)} = -\frac{\omega \bar{U}_1}{\beta^2} \quad \text{and} \quad k_x^{(3)} = k_x^{(4)} = \frac{\omega}{\bar{U}_1}. \tag{18}$$

The eigenspace  $E_{k_x^{(3)}} = \text{Ker}(\mathbf{M} - k_x^{(3)}\mathbf{N})^2$  associated with the eigenvalue  $k_x^{(3)}$  is of dimension 2 and is generated by

$$\mathbf{V}_{c_3} = \left( 0, l, -\frac{\beta}{\bar{U}_1} l, 0 \right)^t \quad \text{and} \quad \mathbf{V}_{c_4} = (0, 0, 0, k)^t, \\ \forall l, k \neq 0.$$

Where subscript ‘‘c’’ corresponds to the critical angle. The eigenspace  $E_{k_x^{(1)}} = \text{Ker}(\mathbf{M} - k_x^{(1)}\mathbf{N})^2$  associated with the eigenvalue  $k_x^{(1)}$  is of dimension 1 only, and is, hence, generated by one vector  $\mathbf{V}_{c_1}$ . Thus, there is no basis in which the matrix  $\mathbf{N}^{-1}\mathbf{M}$  is diagonal ( $\mathbf{N}^{-1}$  is always invertible). The last vector  $\mathbf{V}_{c_2}$  is sought such that the matrix  $\mathbf{N}^{-1}\mathbf{M}$  is in the Jordan form, i.e.,

$$(\mathbf{M} - k_x^{(1)}\mathbf{N})\mathbf{V}_{c_2} = \mathbf{N}\mathbf{V}_{c_1}.$$

Finally,

$$\mathbf{V}_{c_1} = \left( -\frac{\bar{\rho}_1 \bar{c}_1^2}{\bar{U}_1} m, m, -\frac{\beta}{\bar{U}} m, 0 \right)^t, \\ \mathbf{V}_{c_2} = \left( -\frac{\bar{\rho}_1 \bar{c}_1^2}{\bar{U}_1} \left( n + \frac{\beta^4}{\omega \bar{U}_1 \bar{c}_1^2} m \right), \right. \\ \left. n, -\frac{\beta}{\omega \bar{U}_1} (n \omega \bar{U}_1 + m \beta^2), 0 \right)^t, \quad \forall m, n \neq 0.$$

In this basis, the matrix  $\mathbf{N}^{-1}\mathbf{M}$  is given by

$$\mathbf{J} = \begin{pmatrix} -\frac{\omega \bar{U}_1}{\beta^2} & 1 & 0 & 0 \\ 0 & -\frac{\omega \bar{U}_1}{\beta^2} & 0 & 0 \\ 0 & 0 & \frac{\omega}{\bar{U}_1} & 0 \\ 0 & 0 & 0 & \frac{\omega}{\bar{U}_1} \end{pmatrix}. \tag{19}$$

The primitive fluctuating quantities  $(p_c, u_c, v_c, s_c)$  can be found by

$$\mathbf{Z} = \mathbf{P} e^{ix\mathbf{J}} \boldsymbol{\chi}_c,$$

where  $\mathbf{P}$  is the basis transformation matrix, the columns of which are the eigenvectors of matrix  $\mathbf{N}^{-1}\mathbf{M}$  and  $\boldsymbol{\chi}_c$  is the vector  $(C_{c_1}, C_{c_2}, C_{c_3}, C_{c_4})^t$  formed with the integration constants. Ultimately, the general solution of Eq. (9) for the mode  $k_y = \omega/\beta$  is

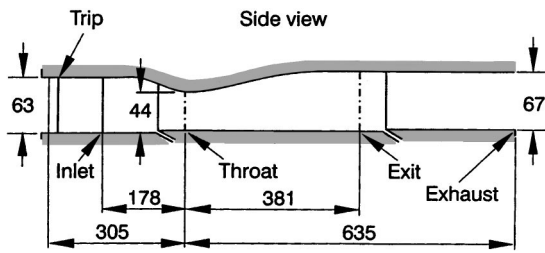


FIG. 8. Sajben and co-workers (see Refs. 12, 13, and 14) diffuser model.

$$\begin{aligned}
 \mathbf{q}_{c_f} = & [(C_{c_1} + ix C_{c_2}) \mathbf{V}_{c_1} e^{ik_x^{(1)}x} + C_{c_2} \mathbf{V}_{c_2} e^{ik_x^{(1)}x} \\
 & + C_{c_3} \mathbf{V}_{c_3} e^{ik_x^{(3)}x} + C_{c_4} \mathbf{V}_{c_4} e^{ik_x^{(3)}x}] E.
 \end{aligned}
 \tag{20}$$

The critical mode thus exhibits an algebraic growth, which comes from the nondiagonal structure of the reduced matrix **J**. Expression (20) for  $x=0$  is then introduced into the linearized relations of Rankine–Hugoniot (8). The following algebraic system is obtained:

$$\mathbf{G}_c \boldsymbol{\chi}_c = \mathbf{F}_c. \tag{21}$$

$\mathbf{G}_c$  is a fourth-order matrix, which depends on  $\omega$  and on the mean flow and  $\mathbf{F}_c$  is the source vector. The determinant of  $\mathbf{G}_c$  is always different from zero, thus  $\boldsymbol{\chi}_c = \mathbf{G}_c^{-1} \mathbf{F}_c$  is always defined. The explicit form of the matrix  $\mathbf{G}_c$ , the vector  $\mathbf{F}_c$ , the analytical expression of the coefficient  $C_{c_j}$ ,  $j=1, \dots, 4$ , and the general form of the solution  $q_{c_f}$  are reported in Appendix C. We are thus able to have relations similar to Eq. (17) but applied to the critical case.

### III. APPLICATIONS

Section II G proves that if there is an emission of acoustic waves in all the admissible directions from a source located downstream of the shock, the shock wave response preferentially to the incident acoustic waves with direction close to  $\theta_{i_c}$  (see Fig. 7).

Under certain conditions, the shock wave in the supersonic flow may exhibit oscillations. As described in the Introduction, this may occur in supersonic diffusers and on transonic airfoils. The next two subsections are devoted to a description of examples for each of the two cases.

#### A. Self-sustained shock oscillations in transonic diffuser flow

##### 1. Diffuser geometry

The major experimental contribution on self-sustained shock oscillations in the diffuser has been achieved by the McDonnell Douglas team headed by Sajben.<sup>12–14</sup> One of the diffusers used in the experiment is asymmetric with a flat bottom wall and a converging–diverging channel. This diffuser is equipped with many suction slots on the vertical walls, so that the flow can be considered two-dimensional, at least in the middle section between the two lateral walls of the channel. Figure 8 gives a sketch of the experimental setup. The diffuser length corresponds to the distance  $l$  between the throat and the exhaust section and is scaled with

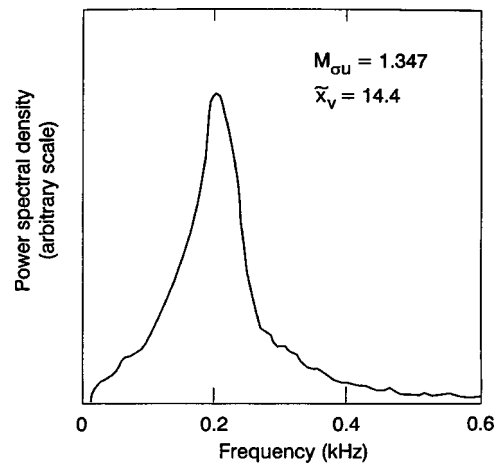


FIG. 9. Shock motion power spectrum in a nozzle, experiment.

the height  $h$  at the throat. In this paper, only the diffuser, with  $l/h \leq 13$ , is studied with the proposed approach.

#### 2. General descriptions

In the considered configuration, the fluid accelerates from a subsonic speed to a supersonic speed through a sonic throat, and is abruptly decelerated by a shock wave located downstream of the throat. The flow is exhausted directly to the ambient air so that the boundary conditions at the exit cross section are closely characterized by a spatially and temporally constant static pressure. The flow conditions are then mainly characterized by the ratio of the static pressure at the exit section to the total pressure at the inlet:  $R_p = p_e/p_t$ . This ratio determines, among other properties, the shock strength and the Mach number  $M_0$  ahead of the shock. The flow patterns obtained with this diffuser depend on the Mach number. In Sajben’s experiment, shock-induced separation occurs for Mach numbers  $M_0$  greater than 1.3 and, in this case, spontaneous self-oscillations have been observed. These oscillations consist of a shock oscillating motion together with the occurrence of fluctuations downstream of the shock. In all cases, no oscillation has been observed in the supersonic zone. The following results are limited to  $R_p = 0.72$  ( $M_0 = 1.34$ ).

#### 3. Experimental results

Among Sajben’s experimental results, the shock motion power spectrum is of particular interest. This spectrum<sup>12</sup> is represented in Fig. 9. It shows that the most sensitive frequencies, for a diffuser length  $l/h = 14.4$ , are close to 200 Hz. Figure 10 shows the experimental results for the iso- $\bar{U}$

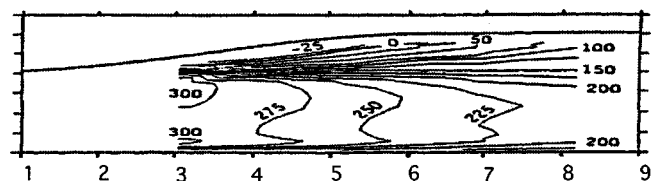


FIG. 10.  $\bar{U}$  contours (m/s), Sajben’s experiment.

contours. On the upper wall, the boundary layer presents a large separation bubble. The reattachment point of the upper boundary layer is located at  $x/h \approx 5$ . As explained before, this point is supposed to be an acoustic source of plane waves.

**4. Simple modeling**

In this paper, the perturbed flow is supposedly inviscid, the present approach is thus limited to the core region where the viscous effects can be neglected. The mean flow is assumed to be constant on both sides of the shock. Although this assumption is not true even at first approximation in the boundary layers and just downstream of the shock, we will show that the knowledge of the upstream Mach number of the shock, the jump relations through shock, and purely geometrical data are sufficient to determine the shock frequency of oscillations and qualitatively some characteristics of the perturbed flow.

The reattachment point emits acoustic waves in all the directions, in particular, with angles close to the critical angle  $\theta_{ic}$ . In Sec. II H, the analytical expression of the fluctuating pressure for  $\theta_i = \theta_{ic}$  has been obtained. All fluctuating quantities are proportional to the shock oscillation amplitude  $X$ , which cannot be determined within the linear analysis. In order to determine the amplitude of the different fluctuating quantities, the fluctuating pressure, for example, must be known somewhere in the flow (normalization). The circular frequency  $\omega$  also is not determined. To determine it, a relation between the shock and the source of the acoustic waves (the reattachment point) must be given. The relation *a priori* chosen consists to suppose that the reattachment point is an extremum for the fluctuating pressure, i.e., an antinode of pressure:

$$\text{Re}[p_f(x_r, y_r, t)],$$

is a pressure antinode if

$$\frac{\partial}{\partial x} \left\{ \cos \left[ \theta_p(x) + \omega \left( -\frac{\bar{U}_1 x}{\beta^2} + \frac{y}{\beta} \right) \right] \right\}_{(x_r, y_r)} = 0,$$

and

$$\frac{\partial}{\partial y} \left\{ \cos \left[ \theta_p(x) + \omega \left( -\frac{\bar{U}_1 x}{\beta^2} + \frac{y}{\beta} \right) \right] \right\}_{(x_r, y_r)} = 0, \tag{22}$$

with  $(x_r, y_r)$  the coordinates of the reattachment point. After some calculations, relations (22) give three possible solutions:

$$\omega = 0, \tag{23a}$$

$$\frac{\text{Im}[f(\bar{q})]}{x_r g(\bar{q})} = \omega \tan \left[ j\pi - \frac{\omega}{\beta} \left( -\frac{\bar{U}_1 x_r}{\beta} + y_r \right) \right], \quad \forall j \in \mathbb{Z}, \tag{23b}$$

$$\omega^2 = -\frac{\beta^2}{\bar{U}_1 [g(\bar{q})]^2} \left[ \text{Im}[f(\bar{q})]g(\bar{q}) + \frac{\bar{U}_1}{\beta^2} [g(\bar{q})]^2 \right] < 0, \tag{23c}$$

$$\forall \bar{M}_0 > 1,$$

with  $f$  and  $g$  given by  $\omega f(\bar{q}) = \mathcal{N}_p$  and  $\omega^2 g(\bar{q}) = \mathcal{M}_p$ , see Appendix C. The only acceptable solution is the relation (23b). It remains to perform a numerical estimation. The upstream mean flow is chosen such that the upstream Mach number and the shock position are realistic (resulting from a stationary Navier–Stokes calculation), the downstream mean flow is calculated through Rankine–Hugoniot relations. In this case, the upstream Mach number is equal to 1.3. The critical angle corresponding to this Mach number is equal to  $\theta_{ic} = \arccos(\bar{M}_1)$ , i.e.,  $\theta_{ic} = 38^\circ$  in the present case. In the Cartesian coordinates system  $Oxy$  fixed on the mean shock, the mean reattachment point coordinates  $(x_r, y_r)$  are (0.12, 0.05), where the origin in  $y$  is on the lower wall. The relation (23b) permits us to find a frequency  $\omega/(2\pi)$  equal to 191.2 Hz ( $j=1$ ). The experimental results of Sajben (Fig. 9) exhibit a well-defined peak close to 210 Hz. The result is not bad, taking into account the numerous assumptions for our approach.

Many theoretical<sup>1</sup> and numerical studies<sup>8</sup> have been performed for the stability analysis of a shock wave or the resolution for the linearized Euler equations, both with the small perturbation technique with a mean flow close to the experimental one. All these studies confirm the present approach for the value of the frequency. Among Sajben’s experimental results, the amplitude and the phase of the pressure fluctuation can be compared to our results. The results are illustrated in the Fig. 11. The results are qualitatively close to the experiment, the amplitude of the fluctuating pressure is roughly constant downstream of the shock and the phase variation is increasing as in the experiment. Nevertheless, the existing differences are related to the assumptions on the mean flow. They are significant in particular immediately downstream of the shock where the flow is strongly dependent on  $x$ , and near the wall, whereas it is, respectively, assumed to be constant and negligible in the present theory. In fact, if the frequency is controlled mainly by a geometrical aspect (reattachment point-shock distance), the boundary layer close to the wall and the nonconstant zone just downstream of the shock, are the weakly extended zone in comparison with the total distance. The approximation of the mean flow by a constant flow is thus quite valid at first approximation. For information, the amplitude and phase evolution of the pressure fluctuation for nonconstant flow are deferred on Fig. 11 (for more details, see Ref. 1). The fast evolution of the pressure fluctuation amplitude close to the shock, where the flow is strongly dependent on  $x$ , is qualitatively found.

**B. Self-sustained oscillations on a wing of a transonic airfoil**

This section is devoted to a validation of the present approach for the shock oscillations inducing the buffeting phenomenon.

**1. Profile geometry and general descriptions**

Two transonic airfoils are considered: the OAT15A-CA airfoil,<sup>6</sup> with a chord of  $c = 200$  mm and CAST 7/DOA1,<sup>15</sup> with a chord of  $c = 100$  mm. The flow on a transonic airfoil

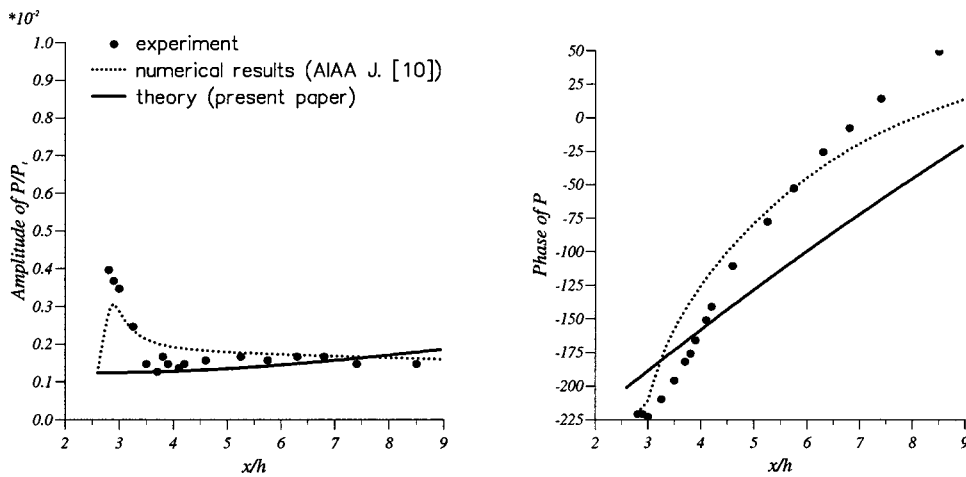


FIG. 11. Nozzle oscillation, amplitude and phase of fluctuating pressure,  $\omega/(2\pi) = 200$  Hz.

is characterized at the design point by the presence of a large supersonic region on the upper surface ended by a shock wave. Increasing the Mach number or the angle of attack beyond the design point leads to the development of stronger shocks which initially only thicken the upper surface boundary layer. However, depending on the severity of the rear adverse pressure gradients, a trailing edge separation may have already developed. A further increase in shock strength causes the boundary layer to separate at the foot of the shock. Again, there may or may not be a trailing edge separation. Raising the angle of attack or the Mach number causes the shock-induced separation bubble to spread downstream while, at the same time, rear separation, may slowly move upstream. Joining together the two separated bubbles usually leads to the beginning of shock oscillations, a condition frequently referred to as airfoil or wing buffet. In our approach, the fluctuations are supposed to be small, i.e., only the beginning of buffeting is accessible to our approach.

**2. Experimental results**

For the airfoil CAST7/DOA1, the available experimental results, which can be compared to our approach, are very few. At the free-stream conditions considered, i.e., a Mach number of  $M_\infty = 0.77$ , an angle of attack of  $\alpha_c = 3^\circ$ , and a Reynolds number of  $Re = 6 \times 10^6$  with the transition fixed at

9% chord, the determined shock oscillation is  $f = 140$  Hz, which is verified by the spectral density distribution depicted in Fig. 12.

For the airfoil OAT15A-CA, there are more experimental results, especially close to the buffeting threshold. The buffeting appears by a very clear increase in the level of pressure fluctuations on the airfoil when the Mach number or the angle of incidence reaches a well-defined limit. With regard to the incidence, this limit is reached for  $\alpha_c = 2.94^\circ$ . Figure 13 shows the fluctuating pressure spectrum downstream of the shock. The shock oscillations are close to 80 Hz, for a Mach number of  $M_\infty = 0.736$ . Figure 14 shows the evolution of the experimental fluctuating pressure coefficient as a function of the airfoil incidence.

**3. Simple modeling**

The theoretical approach is strictly identical to that previously employed. The reattachment point, here the trailing edge, is supposed to be an extremum for the fluctuating pressure. The relation (23b) permits us to obtain the frequency of

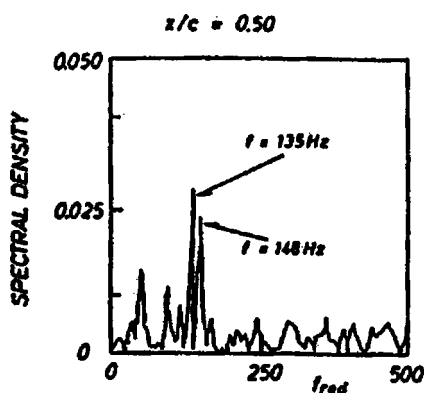


FIG. 12. Spectrum of fluctuating pressure for the critical incidence, CAST7/DOA 1 airfoil, experiment.

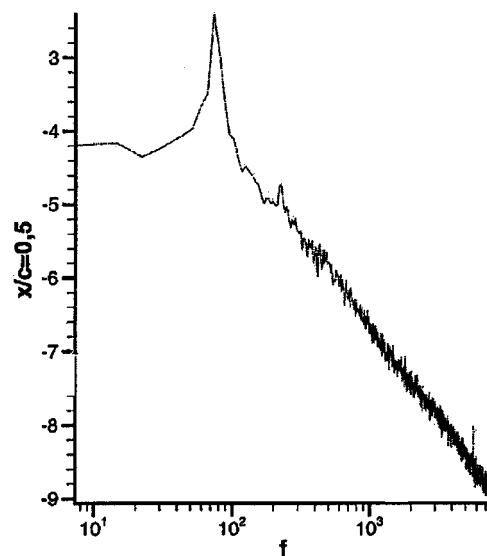


FIG. 13. Spectrum of fluctuating pressure for an incidence of  $\alpha = 2.94^\circ$ , for an abscissa:  $x/c = 0.5$ , OAT15A-200 airfoil, experiment.

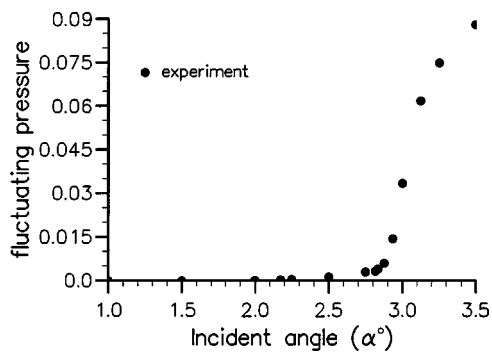


FIG. 14. OAT15A-200 oscillation, evolution of pressure fluctuation vs incident angle.

the oscillation. These results, for the different studied profiles, are summarized in Table I. In Table I, one other airfoil (OAT15A-150) is also presented. The OAT15A-150 airfoil belongs to the same family as airfoil OAT15A-CA but with a chord  $c=150$  mm (for more details, see Ref. 8). Still, in these cases, the present rough modeling permits us to find the characteristic frequency of the oscillations. For the OAT15A-CA airfoil, Figs. 15 and 16 illustrate the comparison between the experimental and theoretical results for the streamwise evolution of the amplitude and the phase of the fluctuating pressure. Experimentally, the amplitude of the pressure fluctuation on the shock position is significant because the shock crosses the sensors. Downstream of the shock, the amplitude is nearly constant. The phase of the pressure fluctuation exhibits a variation of  $135^\circ$  between the mean shock position and 90% of the chord (the reference phase being taken at  $x/c=0.9$ ). The evolution of this phase indicates that the disturbance moves downstream. As in the case of the nozzle, the theoretical predictions are qualitatively close to experiment. The largest difference is close to the shock, where the mean flow is clearly not independent of  $x$  (the assumptions of our modeling are thus not valid any more).

### C. Comments

It remains to determine theoretically the oscillation threshold. One can reasonably suppose that the size of the separated zone plays a fundamental role. Indeed, according to our assumption, if the separation bubble is too small or too wide, the critical angle resulting from the point of separation strikes the shock in a zone where its selectivity is not guaranteed.<sup>1,8</sup> In the nozzle case, if the separated zone is too large, the acoustic waves with a critical angle can “miss” the shock because they will interact with the boundary layer of the opposite wall. Thus, an optimal size of the separated zone must exist so that the acoustic waves resulting from the

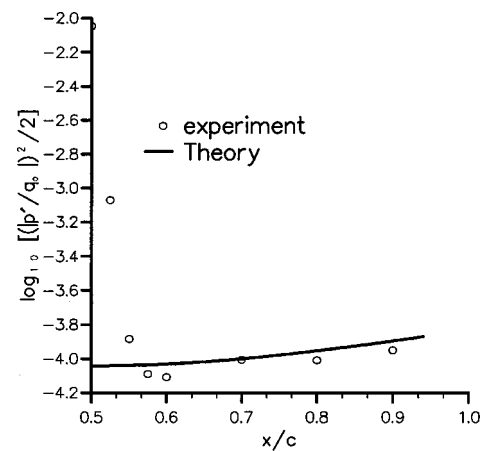


FIG. 15. Comparison between the measured amplitude of the fluctuating pressure for an incidence of  $\alpha=2.94^\circ$  and the theoretical one, upper side, OAT15A-200 airfoil.

activated zone with a critical angle can interact with the shock in an optimal way. These assumptions need to be specified and checked, which will be the subject of future work.

### IV. SUMMARY

The analytical methodology of the present work is based on the study of the interaction of the linear waves with a normal shock wave. The previous studies, Moore,<sup>2</sup> and McKenzie and Westphals,<sup>4</sup> have shown that the reflection coefficient of an acoustic wave downstream of the shock is always lower than 1. However, a critical angle for the incident acoustic wave exists for which the reflection coefficient is equal to 1. At this angle, the shock response is thus marginal. In this paper, this critical angle has been connected to a linearized Euler equation singularity. This singularity corresponds to the case where the incident and the reflected acoustic waves coincide (same frequency, same vector number wave  $\mathbf{k}$  and  $\theta_r = -\pi - \theta_i$ ). From a mathematical point of view, this singularity simply corresponds to the case of the crossing of two eigenvalues branches with, furthermore, an eigenspace of dimension 1 only. Hence, the linearized Euler equation cannot be diagonalized so that the perturbation is no longer a sum of normal modes. The main characteristic of the perturbation is to exhibit an algebraic growth with respect to  $x$ , the  $x$  dependence is of the form:  $(ax+b)e^{ik_x x} E$ . Consequently, if there is in the flow an acoustic source emitting waves in all the possible directions (for example, the reattachment point of the separation bubble), the shock wave preferentially responds to the incident waves close to the critical angle. These results were applied to the case of the shock wave oscillation in a nozzle, then to an airfoil wing.

TABLE I. Data and results for different airfoils.

	Re	$M_\infty$	chord (mm)	$\alpha_c$	$f_{\text{exp}}$	$f_{\text{theo}}$	$(x_r, y_r)$	$\theta_{i_c}$
OAT15A-CA	$4.5 \times 10^6$	0.736	200	$2.94^\circ$	80 Hz	86.3 Hz	(0.08,0)	$37.3^\circ$
OAT15A-150	$6 \times 10^6$	0.73	150	$3.25^\circ$	100 Hz	105.3 Hz	(0.09,0)	$37.1^\circ$
CAST7/DOA1	$6 \times 10^6$	0.77	100	$3^\circ$	140 Hz	133.2 Hz	(0.05,0)	$38.2^\circ$

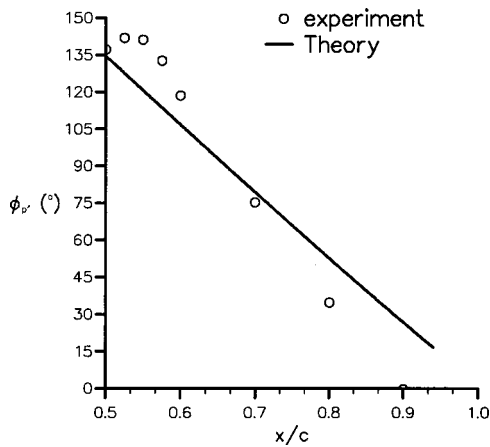


FIG. 16. Comparison between the measured phase of the fluctuating pressure for an incidence of  $\alpha = 2.94^\circ$  and the theoretical one, upper-lower side, OAT15A-200 airfoil.

Indeed, in both cases there is a Mach number threshold beyond which the level of the unsteadiness strongly increases. This threshold generally corresponds to the existence of a massive separation bubble. The reattachment point or the trailing edge is assumed to be the center of strong unsteady activity. There are fluctuations which may arrive on the shock with an angle close to the critical angle. When the present theory is applied, by supposing that the emission point of the fluctuations is a pressure extremum, a relation is

obtained, connecting the frequency of the oscillations to the aerodynamic, thermodynamic  $(\bar{M}_0, \gamma)$ , and geometrical characteristics (related to the distance along the critical angle between the shock and the supposed source of the fluctuations) of the flow. In all the studied cases, the frequency theoretically obtained is close to that measured in the experiments. To our knowledge, it is the first time that a theoretical model can predict successfully the measured shock oscillation frequency. Moreover, certain physical characteristics of the fluctuation (amplitude and phase of the pressure fluctuation) theoretically predicted are compatible with the experimental results. This modeling seems to describe, by a simple mechanism of shock response to an external force, the oscillation of a shock wave on an airfoil or in an over extended nozzle. In future work it seems, however, necessary to extend this approach to nonconstant basic flows in order to specify these results and to describe the space-time evolution of the different fluctuating quantities.

**ACKNOWLEDGMENTS**

This study has been supported by the Center National d’Etudes Spatiales (CNES) and the Office National d’Etudes et de Recherches Aérospatiales (ONERA).

**APPENDIX A: NORMAL MODE**

The matrix **G** and the source vector **F** of the algebraic system (15) are given by

$$\mathbf{G} = \begin{pmatrix} \bar{\rho}_1 \left[ \left( 1 - \frac{\bar{U}_1^2}{\bar{c}_1^2} \right) k_x^{(2)} + \frac{\omega \bar{U}_1}{\bar{c}_1^2} \right] & \bar{\rho}_1 k_y & -\frac{\bar{\rho}_1 \bar{U}_1}{C_p} & \frac{i\omega \bar{\rho}_1}{\bar{U}_0} [\bar{U}] \\ \bar{\rho}_1 \left[ 2\bar{U}_1 k_x^{(2)} - \left( 1 + \frac{\bar{U}_1^2}{\bar{c}_1^2} \right) (\bar{U}_1 k_x^{(2)} - \omega) \right] & 2\bar{\rho}_1 \bar{U}_1 k_y & -\frac{\bar{\rho}_1 \bar{U}_1^2}{C_p} & 0 \\ k_y & -\frac{\omega}{\bar{U}_1} & 0 & -ik_y [\bar{U}] \\ \omega & \bar{U}_1 k_y & \frac{\bar{c}_1^2}{C_p(\gamma-1)} & -i\omega [\bar{U}] \end{pmatrix}, \tag{A1}$$

$$\mathbf{F} = - \begin{pmatrix} \bar{\rho}_1 \left[ (1 - \bar{M}_1^2) k_x^{(1)} + \frac{\omega \bar{M}_1}{\bar{c}_1} \right] \\ \bar{\rho}_1 [2\bar{U}_1 k_x^{(1)} - (1 + \bar{M}_1^2) (\bar{U}_1 k_x^{(1)} - \omega)] \\ k_y \\ \omega \end{pmatrix} C_1. \tag{A2}$$

**APPENDIX B: PROPAGATION CONE**

To try to understand the physical meaning of the propagating cone of acoustic wave in the moving medium, we can use the geometrical acoustic approximation. The geometrical

acoustic approximation consists supposing that the acoustic wave is a plane wave. In general, this is not the case, but when we can suppose that locally the amplitude and the direction of the wave almost do not vary at distances about the wavelength then the approximation of geometrical acoustics

is valid. In this case, we can define the concept of ray as lines whose tangent coincides in each point with the wave propagation direction. We thus have

$$\frac{\partial \mathbf{r}}{\partial t} = \frac{\partial \omega}{\partial \mathbf{k}}, \quad \text{therefore, } \frac{dx}{dt} = \frac{\partial \omega}{\partial k_x} \quad \text{and} \quad \frac{dy}{dt} = \frac{\partial \omega}{\partial k_y}.$$

By dividing these equations one by the other, we obtain

$$\frac{dy}{dx} = \frac{\partial \omega / \partial k_y}{\partial \omega / \partial k_x}. \tag{B1}$$

However, according to the implicit functions rule, we have

$$\frac{\partial k_x}{\partial k_y} = - \frac{\partial \omega / \partial k_y}{\partial \omega / \partial k_x}. \tag{B2}$$

With the relations (B1) and (B2), we can write

$$\frac{dy}{dx} = - \frac{\partial k_x}{\partial k_y}. \tag{B3}$$

In addition,  $k_x^{(1,2)}$  is given by Eq. (10), Eq. (B3) then becomes

$$\frac{dy}{dx} = \pm \frac{\bar{c}_1 k_y}{\sqrt{\omega^2 - k_y^2 (\bar{c}_1^2 - \bar{U}_1^2)}}. \tag{B4}$$

This is the ray equation. We note that when  $k_y > (\omega / \sqrt{\bar{c}_1^2 - \bar{U}_1^2})$ , the rays are not defined. The critical angle thus gives the limit of the geometrical acoustics approximation.

**APPENDIX C: JORDAN MODE**

The matrix  $\mathbf{G}_c$  and the source vector  $\mathbf{F}_c$  of the algebraic system (21) are written as

$$\mathbf{G}_c = \begin{pmatrix} 0 & -\frac{\bar{\rho}_1 \beta^4 m}{\omega \bar{U}_1 \bar{c}_1^2} & \bar{\rho}_1 l & -k \frac{\bar{\rho}_1 \bar{U}_1}{C_p} \\ \frac{\bar{\rho}_1 \beta^2 m}{\bar{U}_1} & -\frac{\bar{\rho}_1 \beta^2}{\omega \bar{U}_1^2} \left[ \beta^2 m \left( 1 + \frac{\bar{U}_1^2}{\bar{c}_1^2} \right) + \bar{U}_1 \omega n \right] & 2\bar{\rho}_1 \bar{U}_1 l & -\frac{\bar{\rho}_1 \bar{U}_1^2 k}{C_p} \\ -\frac{\beta m}{\bar{U}_1} & -\frac{(m\beta^2 + n\omega \bar{U}_1)}{\omega \bar{U}_1^2} \beta & -\frac{\beta l}{\bar{U}_1} & 0 \\ -\frac{\beta^2 m}{\bar{U}_1} & -\frac{(\beta^2 m + n\omega \bar{U}_1)}{\omega \bar{U}_1^2} \beta & \bar{U}_1 l & \frac{\bar{c}_1^2 k}{C_p(\gamma - 1)} \end{pmatrix}, \tag{C1}$$

$$\mathbf{F}_c = \begin{pmatrix} -\frac{i\omega \bar{\rho}_1}{\bar{U}_0} [\bar{U}] \\ 0 \\ ik_y [\bar{U}] \\ i\omega [\bar{U}] \end{pmatrix} X. \tag{C2}$$

After some calculations, an analytical expression of the coefficient  $C_{c_j}$ , ( $j=1, \dots, 4$ ) is obtained:

$$\begin{aligned} C_{c_1} &= - \frac{i[\bar{U}]((\gamma - 1)\bar{c}_1^2 \bar{U}_1 [\bar{U}] + \bar{U}_0 \bar{U}_1 \beta^2 + \bar{U}_1^4 - \bar{c}_1^4 - 2\bar{U}_1^2 \bar{c}_1^2)}{\bar{U}_0 \bar{c}_1^2 \beta^2 m} \omega X - \frac{n}{m} C_{c_2}, \\ C_{c_2} &= \frac{i\bar{U}_1 [\bar{U}] [(\gamma - 1)\bar{U}_1 [\bar{U}] + \bar{U}_0 \bar{U}_1 - (\bar{c}_1^2 - \bar{U}_1^2)]}{\bar{U}_0 \beta^4 m} \omega^2 X, \\ C_{c_3} &= - \frac{i\bar{U}_1 [\bar{U}]^2}{\bar{U}_0 \bar{c}_1^2 l} \omega X, \\ C_{c_4} &= \frac{iC_p(\gamma - 1)[\bar{U}]^2}{\bar{U}_0 \bar{c}_1^2 k} \omega X. \end{aligned} \tag{C3}$$

Finally, the general solution (20) is

$$\begin{aligned}
 p_{c_f}(x, y, t) &= \mathcal{R}_p(x, \omega, \bar{q}) e^{i[\theta_p(x) + \omega(-(\bar{U}_1/\beta)^{1/2}x + (y/\beta) - t)]} X, \\
 u_{c_f}(x, y, t) &= \mathcal{R}_u^{(a)}(x, \omega, \bar{q}) e^{i[\theta_u(x) + \omega(-(\bar{U}_1/\beta)^{1/2}x + (y/\beta) - t)]} X \\
 &\quad + \mathcal{R}_u^{(v)}(\omega, \bar{q}) e^{i[(\pi/2) + \omega((x/U_1) + (y/\beta) - t)]} X, \\
 v_{c_f}(x, y, t) &= \mathcal{R}_v^{(a)}(x, \omega, \bar{q}) e^{i[\theta_v(x) + \omega(-(\bar{U}_1/\beta)^{1/2}x + (y/\beta) - t)]} X \\
 &\quad + \mathcal{R}_v^{(v)}(\omega, \bar{q}) e^{i[(\pi/2) + \omega((x/U_1) + (y/\beta) - t)]} X,
 \end{aligned} \tag{C4}$$

$$s_{c_f}(x, y, t) = \mathcal{R}_s(\omega, \bar{q}) e^{i[(\pi/2) + \omega((x/U_1) + (y/\beta) - t)]} X,$$

with

$$\begin{aligned}
 \bullet \mathcal{R}_p(x, \omega, \bar{q}) &= \sqrt{(x\mathcal{M}_p)^2 + [\text{Im}(\mathcal{N}_p)]^2}, \\
 \theta_p(x) &= \arctan\left(\frac{\text{Im}(\mathcal{N}_p)}{x\mathcal{M}_p}\right),
 \end{aligned}$$

with

$$\begin{aligned}
 \mathcal{M}_p &= -i \frac{\bar{\rho}_1 \bar{c}_1^2}{\bar{U}_1} m C_{c_2}, \\
 \mathcal{N}_p &= -\left(\frac{\bar{\rho}_1 \bar{c}_1^2}{\bar{U}_1} (m C_{c_1} + n C_{c_2}) - \frac{\bar{\rho}_1 \beta^4}{\bar{U}_1^2 \omega} m C_{c_2}\right),
 \end{aligned}$$

$$\begin{aligned}
 \bullet \mathcal{R}_u^{(a)}(x, \omega, \bar{q}) &= \sqrt{(x\mathcal{M}_u)^2 + [\text{Im}(\mathcal{N}_u)]^2}, \\
 \theta_u(x) &= \arctan\left(\frac{\text{Im}(\mathcal{N}_u)}{x\mathcal{M}_u}\right),
 \end{aligned}$$

with

$$\begin{aligned}
 \mathcal{M}_u &= i m C_{c_2}, \quad \mathcal{N}_u = m C_{c_1} + n C_{c_2}, \\
 \mathcal{R}_u^{(v)}(\omega, \bar{q}) &= \text{Im}(l C_{c_3})
 \end{aligned}$$

$$\begin{aligned}
 \bullet \mathcal{R}_v^{(a)}(x, \omega, \bar{q}) &= \sqrt{(x\mathcal{M}_v)^2 + [\text{Im}(\mathcal{N}_v)]^2}, \\
 \theta_v(x) &= \arctan\left(\frac{\text{Im}(\mathcal{N}_v)}{x\mathcal{M}_v}\right),
 \end{aligned}$$

with

$$\begin{aligned}
 \mathcal{M}_v &= -i \frac{\beta}{\bar{U}_1} m C_{c_2}, \\
 \mathcal{N}_v &= -\frac{\beta}{\bar{U}_1} \left( m C_{c_1} + n C_{c_2} + \frac{\beta^2}{\omega \bar{U}_1} m C_{c_2} \right), \\
 \mathcal{R}_v^{(v)}(\omega, \bar{q}) &= \frac{\beta}{\bar{U}_1} \text{Im}(l C_{c_3}), \\
 \bullet \mathcal{R}_s &= \text{Im}(k C_{c_4}).
 \end{aligned}$$

<sup>1</sup>J.-Ch. Robinet and G. Casalis, "Shock oscillation in diffuser modeled by a selective noise amplification," *AIAA J.* **37**, 453 (1999).  
<sup>2</sup>F. K. Moore, "Unsteady oblique interaction of a shock wave with a plane disturbance," NACA Report No. 1165 (1954).  
<sup>3</sup>H. S. Ribner, "Cylindrical sound wave generated by shock-vortex interaction," *AIAA J.* **23**, 1708 (1984).  
<sup>4</sup>J. F. McKenzie and K. O. Westphal, "Interaction of linear waves with oblique shock waves," *Phys. Fluids* **11**, 2350 (1968).  
<sup>5</sup>K. Mahesh, S. Lee, S. Lele, and P. Moin, "The interaction of an isotropic field of acoustic waves with a shock wave," *J. Fluid Mech.* **300**, 407 (1995).  
<sup>6</sup>O. Reberga, "Etude theorique et experimentale de dispositifs de controle actif d'instabilites en ecoulement transsonique avec onde de choc," Ph.D. thesis, These ENSAE (2000).  
<sup>7</sup>J. Ch. Robinet, J. Gressier, G. Casalis, and J. M. Moschetta, "Shock wave instability and carbuncle phenomenon: Same intrinsic origin?" *J. Fluid Mech.* **417**, 237 (2000).  
<sup>8</sup>J.-Ch. Robinet, "Stabilité lineaire d'un ecoulement presentant une onde de choc," Ph.D. thesis, École Nationale Supérieure de l'Aéronautique et de l'Espace (1999).  
<sup>9</sup>H. S. Ribner, "Convection of a pattern of vorticity through a shock wave," NACA Technical Note No. 2864 (1954).  
<sup>10</sup>B. Hardy and H. M. Atassi, "Interaction of acoustic, entropic and vortical waves," *AIAA Paper No. 97-1614* (1997).  
<sup>11</sup>T. A. Zang, M. Y. Hussaini, and D. M. Bushnell, "Numerical computations of turbulence amplification in shock-wave interactions," *AIAA J.* **22**, 13 (1984).  
<sup>12</sup>T. J. Bogar, M. Sajben, and J. C. Kroutil, "Characteristic frequencies of transonic diffuser flow oscillations," *AIAA J.* **21**, 1232 (1983).  
<sup>13</sup>M. Sajben T. J. Bogar, and J. C. Kroutil, "Characteristic frequency and length scales in transonic diffuser flow oscillations," *AIAA 14th Fluid and Plasma Dynamics Conference*, No. AIAA-81-1291 (1981).  
<sup>14</sup>M. Sajben and T. J. Bogar, "Unsteady transonic flow in a two-dimensional diffuser: Interpretation of experimental results," Report McDonnell Douglas Corp., Report No. MDC Q0779 (1982).  
<sup>15</sup>E. Stanewsky and D. Basler, "Mechanism and Reynolds number dependence of shock-induced buffet on transonic airfoils," in *IUTAM Symposium Transsonicum III, Berlin*, (Springer, Berlin, 1989), pp. 479-488.